Tellus (1988), *40A*, 61–79

Semi-geostrophic flow of a stratified atmosphere over elongated isentropic valleys and ridges

By HUW C. DAVIES and JOSEF HORN, *Atmospheric Physics, ETH, CH-8093 Zürich, Switzerland*

(Manuscript received July 9, 1986; in final form February 16, 1987)

ABSTRACT

A study is undertaken of semi-geostrophic flow of a stratified inviscid atmosphere over various forms of infinite (and some forms of finite) length isentropic orographic features on an f-plane. Finite-amplitude, explicit solutions are derived under the stipulation that the velocity (U) and the Brunt Väisälä frequency (N) of the upstream flow are both uniform.

In the case of the infinite ridge configuration, it is shown that, in contrast to the case of orographically forced buoyancy waves where breakdown is associated with the waves attaining a vertical tilt, the breakdown of semi-geostrophic flow is accompanied by a local fusion of the isentropes at the surface with an associated infinite across-ridge flow. The criteria for, and the spatial location of, the breakdown are demonstrated to be sensitively dependent upon the dimensionless Rossby radius of deformation (NH/fL) and the "orographic shape". (Here H and L refer to the characteristic height and width of the ridge.) In particular, the separate influence upon the flow of the curvature and the asymmetry of the orography is explored. It is shown that large convex curvature enhances the likelihood of flow breakdown and that an asymmetric valley-ridge profile is accompanied by a non-zero mean along-ridge flow component but with no attendant net Coriolis lift.

Three-dimensional solutions are derived for flow over some special, "zero net volume" forms of orography. In addition to the breakdown of semi-geostrophy, the flow response can also exhibit a Taylor cone structure. The criterion for the cone's existence is related to the value of a Froude number (defined in terms of the amplitude of the cross-ridge flow component of the incident flow).

Attention is also drawn to the formal limitation of semi-geostrophy and some consideration is given to the implications of its violation.

1. Introduction

The use of the term mesoscale in a meteorological context usually carries with it a connotation of an interjacent scale. In the case of adiabatic atmospheric flow over mesoscale two-dimensional ridges such an inference is fully justified. Theoretical studies of this flow configuration in the limit of infinitesimal amplitude orography (see e.g. Queney, 1947, 1948; Eliassen, 1968; Smith, 1979a; Pierrehumbert, 1984) underscore this scale as a transition-zone in parameter space between the quasi-geostrophic, hydrostatic flow response to macro-scale ($L \gg 600$ km) orographic forcing and the predominantly ageostrophic, non-hydrostatic response to microscale ($L \ll 6$ km) surface undulations.

In this study our interest lies primarily at the upper end of the mesoscale ($L \sim 100$–600 km) for which the Rossby number, $R_0 = U/fL$, defined in terms of the far upstream flow speed (U) is such that $R_0 \lesssim 1$. On this scale the foregoing studies using linear theory indicate that some key aspects of the flow dynamics are sensitive to the value of the Rossby number. For example the inequalities $\{R_0 \gg 1; R_0 \ll 1\}$ demark respectively the regimes characterized by, on the one hand a vertically evanescent, essentially geostrophic orographic flow response, and on the other hand the generation of appreciable vertically propagating buoyancy-inertia waves that possess an upstream phase tilt with height and an accompanying substantial surface pressure drag. For $R_0 \sim 1$ these studies suggest that both the geostrophic and ageostrophic signals should be evident in the flow response.

The influence in the $R_0 \sim 1$ limit of finite amplitude orography has been the subject of examination in a range of numerical model studies (Eliassen and Rekustad, 1971; Mason and Sykes, 1978; Eliassen and Thorsteinsson, 1984; Pierrehumbert and Wyman, 1985). Eliassen and Thorsteinsson's results illustrate that the generation and the spatial structure of the buoyancy-inertia waves is dependent upon the prevailing Rossby number of the low-level flow field and the "effective-transmissivity" of these waves in the incident flow field. Pierrehumbert and Wyman (1985) explored in some detail the relationship between the characteristic value of the inverse Froude number ($\mathscr{F} = NH/U$) of the far upstream incident flow and the formation of a low-level blocked region upstream. Here N and H denote respectively the Brunt-Väisälä frequency and a mountain height scale. These results suggest that finite orographic amplitude enhances the upstream deacceleration and that at some finite value of $\mathscr{F}(\sim 1)$ there is an onset of low-level upstream flow blocking. This tends to occur prior to, or is accompanied by, the occurrence of buoyancy wave overturning in an elevated layer located somewhat downstream of the crest.

Recourse to simple theoretical models to provide further understanding of these flow phenomena in the $R_0 \sim \mathscr{F} \sim 1$ part of parameter space is hampered by the inevitable non-linearity implied by these criteria. However, some insight can be gleaned by backtracking and resorting to the study of semi-geostrophic, adiabatic flow over infinitely long ridges. In the present context we take the semi-geostrophic assumption to refer to flows with geostrophy assumed only for the along-ridge flow component. In essence the introduction of this approximation curtails the validity of the system to some region below the $R_0 = 1$ divide in parameter space, and concomitantly it implies that the dynamical constraint imposed on the airflow by the earth's rotation remains moderately strong. The resulting flow field is balanced, but not necessarily quasi-geostrophic.

The present study is confined exclusively to this finite-amplitude, semi-geostrophic limit. Furthermore we make the following trenchant assumptions: the orographic surface is isentropic, the atmosphere semi-infinite but essentially incompressible and the incident airstream possesses a uniform flow speed (U) and a constant Brunt-Väisälä frequency (N). Within this framework we derive analytical solutions for a class of infinitely long orographic valley and ridge systems and also for some special elongated but finite terrain features.

Thus the present work is complementary to, and forms a bridge between, two previous types of theoretical studies: The examination of quasi-geostrophic stratified flow over finite length and width obstacles (e.g. Hogg, 1973; Huppert, 1975; Buzzi and Speranza, 1979; Smith, 1979b; Bannon, 1986), and the group of studies of semi-geostrophic flow over infinite ridges (Robinson, 1960; Jacobs, 1964; Merkine, 1975; Davies et al., 1984; Pierrehumbert, 1985).

In the former group of studies, the salient physical process governing the flow response arises from the contraction of vortex filaments as the fluid mounts the obstacle. For the standard case of an uniform airstream of constant static stability in a vertically unbounded atmosphere, the resulting orographically induced anticyclonic vortex decays with height like $\exp\{-Nz/f\}$. If the orography is high enough a stagnation point occurs somewhere on the fringe of the mountain. The associated closed streamline at the surface is surmounted by a Taylor cone. A stringent limitation on the validity of the solutions derived with this approach is the restriction of the flow to quasi-geostrophy and hence usually to small obstacle heights.

In the second type of study, there is not such a severe constraint upon the mountain amplitude. The adoption of the semi-geostrophic approximation coupled with a coordinate transform to: a system with a stream function vertical coordinate (Robinson, Pierrehumbert), an isentropic vertical coordinate (Jacobs, Davies et al.) or geostrophic space (Merkine), has facilitated the derivation of a small number of finite-amplitude analytical solutions. The results obtained indicate that the features of the overall flow structure are, not unexpectedly, similar to the corresponding geostrophic response (Buzzi and Tibaldi, 1977; Smith, 1979b). The major dynamical influence is again the sequence "extension-contraction-extension" of vortex filaments as the fluid traverses the ridge, i.e., relative to the far upstream pattern the separation of neighbouring isentropic surfaces increases ahead of and behind the ridge but diminishes in the neighbourhood of the crest. However, for high crest elevations, the amplitude of the diminution at the crest far surpasses that of the off-crest broadening. Thus it follows that the flow speed-up and anticyclonic vorticity over the crest is more evident than the reduction of the normal velocity component and the generation of cyclonic vorticity elsewhere. In addition it has been shown that in the case of a semi-infinite atmosphere and bell-shaped finite amplitude ridge there is flow breakdown if the dimensionless parameter combination $R_0 \mathscr{F} = (NH/fL)$ exceeds the critical value of 1 (Davies et al., 1984; Pierrehumbert, 1985; hereafter these studies are referred to respectively as D and P). This is a rather severe criterion for synoptic/meso-scale orography, and the refinement and implications of the criterion will form one theme of the present study. The breakdown is associated with a fusion of adjacent isentropes at the ridge crest and a consequent infinite value for the across-ridge velocity component. In addition, in P, the surface distribution for several other orographic profiles was deduced and one of these included a piecewise continuous triangular orographic profile. For the latter, non-smooth profile, flow breakdown occurred for all values of $(R_0 \mathscr{F})$.

The amalgam of the two foregoing types of studies, i.e., semi-geostrophic flow over three dimensional orography, has been previously discussed by Merkine and Kalnay Rivas (1976) and Davies and Roth (1986). The latter study is analogous to the present one except that a shallow water system was considered. For this system the two-dimensional problem does not involve a logarithmic far field behaviour and it is possible in principal to treat a wide class of "local" orographic features. In effect the shallow water and continuous stratification systems are dynamically distinct (c.f., Huppert, 1975). On the other hand Merkine and Kalnay Rivas considered the flow over three-dimensional orography using the full "geostrophic momentum" set of equations. Thus their work and the results of the present section constitute different approaches to the study of finite amplitude "balanced" but not necessarily geostrophic flow over orography. Their approach is appropriate for almost-symmetrical obstacles and ours to elongated terrain.

In Section 3 of the present study, we present a set of explicit closed form solutions for the two-dimensional problem. This set further illustrates the nature of the balanced flow response in the $R_0 \to 1$ limit, and concomitantly helps isolate the factors that induce the flow breakdown.

Aspects of the flow over elongated, but finite length, orographic features are considered in Section 4. The results of the previous section are utilized and extended to provide semi-geostrophic solutions for flow over three-dimensional isentropic orography configurations that possess a zero mean volume. Thus in the apposite categorization of Eliassen (1980) this part of our study is confined to the "isentropic-open" and "isentropic-closed" flow configurations. The former case corresponds to the advancing surface flow rising over the crest. In the second case there is a stagnation point somewhere on the ridge with an associated closed streamline and, as noted earlier, a Taylor-cone effect.

In Section 5, attention is directed toward the limitations of the derived semi-geostrophic solutions and to the implications of these limitations.

2. The flow model

The starting point for our analysis is the set of equations governing steady, adiabatic, hydrostatic flow of an inviscid, anelastic Boussinesq fluid on an f-plane. In an isentropic coordinate system, and on invoking an incompressibility condition, these equations take the compact form,

$$\left.\begin{aligned} Du - fv &= -M_x, && \text{(a)}\\ Dv + fu &= -M_y, && \text{(b)}\\ M_\theta &= -gz/\Theta, && \text{(c)}\\ (M_{\theta\theta} u)_x + (M_{\theta\theta} v)_y &= 0, && \text{(d)} \end{aligned}\right\} \quad (2.1)$$

where

$$M = \{p/\rho_0 - g\theta z/\Theta\},$$

is the equivalent for an incompressible fluid of the conventional Montgomery function. Here (ρ_0, Θ) refer to the constant base values for the "density" and potential temperature of a quiescent basic state. The variable M is defined relative to these base values. The subscripts (x, y) refer to derivatives on θ surfaces and D is the advective operator on these isentropic surfaces, i.e.

$$D = \left\{u \frac{\partial}{\partial x} + v \frac{\partial}{\partial y}\right\}.$$

This set of equations is equivalent (except for sign changes) to the usual incompressible α coordinate system utilized by Eliassen (1980). In the present study we consider an airstream incident upon various two-dimensional or elongated orographic ridges/valleys aligned along the y-axis. The incident stream is assigned an uniform velocity field $(U, V) = (\mathscr{V} \sin \alpha, \mathscr{V} \cos \alpha)$ i.e. $\alpha \to 0$ and $\alpha \to \pi/2$ correspond respectively to an acute and a normal angle of attack of the incident flow. Also we assign to the incident flow a uniform stratification with a constant Brunt-Väisälä frequency (N).

It will prove helpful to introduce a partition of the M and z variables of the set (2.1) into their far-upstream values $(\mathscr{M}, Z)$ and their deviations therefrom (m', z'). The upstream values incorporate both the contribution associated with the mean stratification and a component balancing the far field geostrophic flow, i.e.,

$$M = \mathscr{M} + m', \qquad z = Z + z',$$

with

$$\mathscr{M} = -\tfrac{1}{2}(g/\Theta)\left(\frac{\partial Z}{\partial \theta}\right)\theta^2 - f\mathscr{V}(y \sin \alpha - x \cos \alpha),$$

$$Z = (g/\Theta)\, N^{-2}\,\theta.$$

Now consider the rationale for introducing the semi-geostrophic assumption. Horizontal anisotropy is a frequent feature of the earth's sub-synoptic/meso-α scale mountain ranges. On this scale a conventional Rossby number based upon the characteristic width of the orography will not be small compared with unity. However some form of balanced flow will still prevail provided the acceleration associated with individual fluid elements is small relative to the Coriolis acceleration, i.e., provided the particle trajectories traverse sufficiently slowly through the flow regions of strong spatial variability. This is the essence of the semi-geostrophic approximation. For elongated topography we expect $|Du| \approx |uu_x|$, and we postulate that $|(u_x/f)\cdot(u/v)| \ll 1$, and hence replace (2.1a) by the geostrophic relation,

$$fv = M_x \tag{2.1a'}$$

The closed form nature of the solutions presented later enable us to undertake explicit *à posteriori* examination of the validity of the assumption.

In terms of the deviation variables (m', z'), the eqs. (2.1a', 2.1b–d) take the form

$$\left.\begin{aligned} fv &= m'_x + f(\mathscr{V} \cos \alpha), && \text{(a)}\\ Dv + fu &= -m'_y + f(\mathscr{V} \sin \alpha), && \text{(b)}\\ m'_\theta &= -(g/\Theta)\, z', && \text{(c)}\\ (M_{\theta\theta} u)_x + (M_{\theta\theta} v)_y &= 0. && \text{(d)} \end{aligned}\right\} \tag{2.2}$$

This reduced set possesses the following potential vorticity conservation relationship

$$D(\mathscr{P}) = 0 \tag{2.3a}$$

where

$$f\mathscr{P} = (m'_{xx} + f^2)/M_{\theta\theta},$$

and in the far-field $f\mathscr{P} = f^2/\mathscr{M}_{\theta\theta}$, i.e. the potential vorticity is uniform. It then follows from (2.2c) and (2.3b) that z', the deviation of the isentropic surfaces from their far-field values satisfies the differential equation

$$z'_{xx} + \mu^2 z'_{\theta\theta} = 0, \tag{2.4}$$

where

$$\mu^2 = -f^2/\mathscr{M}_{\theta\theta}.$$

This equation is to be solved subject to the boundary conditions

$$z'(x, y, 0) = \eta(x, y), \tag{2.5a}$$

and

$$z'(x, y, \theta) \to 0 \qquad \text{as} \qquad \theta \to \infty. \tag{2.5b}$$

Note that eq. (2.4) is equivalent to eq. (4.9) of Eliassen (1980) where it is used to describe a topographically bound flow induced by an infinite ridge without a general current. The complete flow field can be determined from the solution of the system (2.4–2.5) for z', using successively (2.2c, a, d) to evaluate M, v and u. This solution sequence serves to emphasize that in any (x, θ) section the solutions for z' and v are independent of the along-ridge variation of the orographic profile. Thus the three-dimensionality of the flow structure is directly linked to the variations from one (x, θ) section to another of the (z', v) fields. The induced ageostrophic across-ridge flow component merely serves to maintain the geostrophy of the along-ridge flow. It will become apparent later that this implicit nature of the u field dependency will impose a restriction on the type of finite length ridges we can consider. Also note that it is our adoption of an isentropic coordinate system that allows us to extend the study to the consideration of elongated but finite ridges.

A variety of solutions of the above system will be derived in the subsequent sections, and it is thus appropriate to perform a non-dimensionalisation. First we introduce the following dimensionless variables,

$$\tilde{x} = x/L, \quad \tilde{y} = y/\mathscr{L}, \quad \tilde{\theta} = g\theta/(N^2 H\Theta),$$
$$\tilde{m} = m'/\mathscr{V}^2, \quad \varphi = z'/H, \quad (\tilde{u}, \tilde{v}) = (u, v)/\mathscr{V}. \tag{2.6}$$

Note that the independent variable $\tilde{\theta} \equiv Z/H$, where Z refers to the height of the undisturbed θ-surface above the flat terrain.

Three important dimensionless combinations that arise naturally for this problem are the Rossby number (R_0), an inverse Froude number ($\mathscr{F}$) and an orographic anisotropy parameter (R_L). These are defined by

$$R_0 = \mathscr{V}/fL, \qquad \mathscr{F} = NH/\mathscr{V}, \qquad R_L = \mathscr{L}/L.$$

Many dimensionless numbers are formulated essentially as the ratio of an inertial effect to some other effect, e.g., the Rossby number, Reynolds number and the usual Froude number. Recently the use of the inverse of the Froude number has been adopted/advocated (see Pierrehumbert and Wyman, 1985; Baines and Hoinka, 1986) on the basis that it constitutes one natural measure of the non-linearity in the case of stratified flow over orography. Our use of $\mathscr{F}$ in the present study, where it frequently occurs in tandem with R_0, is based at least partly upon notational convenience.

In terms of the new variables the eqs. (2.4–2.5) take the form

$$(R_0\mathscr{F})^2 \varphi_{\tilde{x}\tilde{x}} + \varphi_{\tilde{\theta}\tilde{\theta}} = 0, \tag{2.7}$$

with

$$\varphi(\tilde{x}, \tilde{y}, 0) = \tilde{\eta}(\tilde{x}, \tilde{y}),$$
$$\varphi(\tilde{x}, \tilde{y}, \tilde{\theta}) \to 0 \quad \text{as} \quad \tilde{\theta} \to \infty. \tag{2.8}$$

The corresponding forms for the potential vorticity relationship (2.3), the hydrostatic relationship (2.2c), and the across-ridge flow component are

$$R_0 \tilde{v}_{\tilde{x}} = \varphi_{\tilde{\theta}}, \tag{2.9}$$
$$\tilde{m}_{\tilde{\theta}} = -\mathscr{F}^2 \varphi, \tag{2.10}$$
$$u = (1 + \varphi_{\tilde{\theta}})^{-1}[\sin\alpha - (R_0/R_L)(\tilde{v}\tilde{v}_{\tilde{y}} + \tilde{m}_{\tilde{y}})]. \tag{2.11}$$

Note that, in accord with our previous remarks, it is only the cross-ridge flow component that exhibits a dependency upon the flow angle (α) and the orographic anisotropy parameter R_L. It also follows from (2.11) that an orographic profile with a zero amplitude at a given y-section will not generate a flow response at that section. Thus, for the present semi-geostrophic limit, the response of a finite length orography is confined to the lateral domain of the orography.

3. Flow over two-dimensional valleys and ridges

Here we present several compact closed form solutions for flow incident normally (i.e., $\alpha \equiv \pi/2$) upon infinitely long ($R_L^{-1} \equiv 0$) ridges. Our purpose is two-fold: to embellish and extend the previous studies of the same problem and to prepare the ground work for the study of the three-dimensional problem in the next section.

3.1. *Witch of Agnesi orography*

Consider the Witch of Agnesi orographic profile,

$$\tilde{\eta} = 1/(1 + \tilde{x}^2).$$

Note that the horizontal and vertical scaling is such that the L and H of the non-dimensionalization (2.6) correspond to the half-width and the ridge height. For this profile the solution of the problem posed by (2.7–2.8) is derived using the usual Fourier transform procedures. It takes the form

$$\varphi(\tilde{x}, \tilde{\theta}) = \delta/(\delta^2 + \tilde{x}^2), \tag{3.1}$$

where

$$\delta = \{1 + (R_0\mathscr{F})\tilde{\theta}\}.$$

The accompanying along- and cross-ridge flow components are evaluated using (2.9–2.11), and they are given by

$$\tilde{v}(\tilde{x}, \tilde{\theta}) = -\mathscr{F}\tilde{x}/(\delta^2 + \tilde{x}^2), \tag{3.2}$$

$$\tilde{u}(\tilde{x}, \tilde{\theta}) = \{1 - R_0\mathscr{F}(\delta^2 - \tilde{x}^2)/(\delta^2 + \tilde{x}^2)^2\}^{-1}. \tag{3.3}$$

Aspects of the surface distribution of these solutions were given previously in D and P. Fig. 1 displays the structure of the full fields. They resemble the familiar quasi-geostrophic features with comparatively strong anti-cyclonic vorticity (decrease in the isentrope separation) straddling the crest, and weaker and more widespread

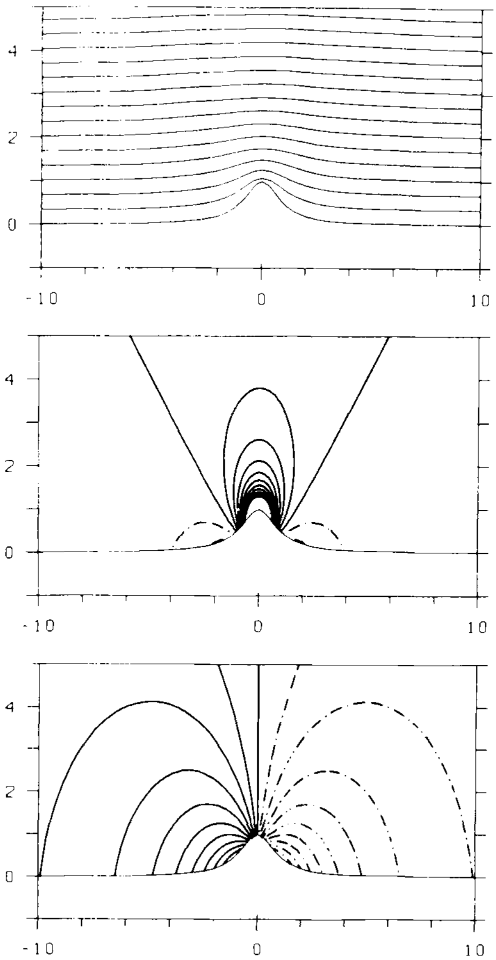

Fig. 1. Semi-geostrophic, two-dimensional flow fields over Witch of Agnesi orography. The panels display respectively the structure of the isentropes, the u and the v fields (in dimensionless units) for $R_0\mathscr{F} = 0.99$. (Breakdown of solution occurs at $R_0\mathscr{F} = 1$.) The flow approaches from the left and positive v-values are related to flow into the section. The lowest isentrope is equivalent to the specified orography. Velocity isolines are displayed at intervals of 0.05 and dashed isolines correspond to negative perturbations.

cyclonic vorticity (increase in isentrope separation) on either side. It follows from (3.3) that the flow solutions breakdown at the crest as the parameter $(R_0\mathscr{F})$ approaches unity from below. In essence as this limit is approached the vortex contraction over the crest increases with an accompanying increase in the value of the static stability, and the cross-ridge flow speed intensifies in an unbounded manner. However, it needs to be noted that the primary mathematical foundation for the solutions, i.e. the semi-geostrophy assumption, will have formally been violated prior to the breakdown. The ratio

$$E = |uu_x|/|fv|.$$

is one measure of the credibility of the semi-geostrophic assumption. In the present case the surface value of this ratio is given by

$$E(\tilde{x}, 0) = |2R_0^2(3 - \tilde{x}^2)(1 + \tilde{x}^2)^{-2} \{1 - R_0\mathscr{F}(1 - \tilde{x}^2)/(1 + \tilde{x}^2)^2\}^{-3}|. \quad (3.4)$$

A credibility requirement of the form $E \ll 1$ for the solutions demands that

$$R_0^2 \ll 1 \quad \text{at} \quad (1, 0),$$
$$6R_0^2(1 - R_0\mathscr{F})^{-3} \ll 1 \quad \text{at} \quad (0, 0).$$

Thus the acceptance of such a requirement would imply that the semi-geostrophic solution (3.1–3.3) would cease to be acceptable much prior to $(R_0\mathscr{F}) \to 1$. We shall comment further in Section 5 on some of the implications of this result.

Note also that the formulae (3.1–3.3), with appropriate and trivial modification, also incorporate the solution for flow over a valley. In this case there is deacceleration over the trench bottom and mild acceleration far up and downstream. Flow breakdown would now be associated with the far field acceleration. This would require considerably higher values of $(R_0\mathscr{F})$. Also the foregoing credibility requirements, now with $\mathscr{F}$ replaced by $-\mathscr{F}$ are far less restrictive. An example of the flow response to a valley is given in Fig. 2. A strong tendency for along-valley flow channelling is evident. Note that for the two-dimensional orography considered in this section we can infer from (2.2b) that the link between the two horizontal velocity components is given by

$$v_x = f(U/u - 1). \quad (3.5)$$

It is also pertinent to note that a finite domain numerical model simulation of this flow configuration would entail a determination of the lateral boundary flow conditions. In the steady state far field there is a geostrophically balanced along-ridge component, and this would either have to be specified *à priori* and externally, or computed internally as the flow evolved from an initial state.

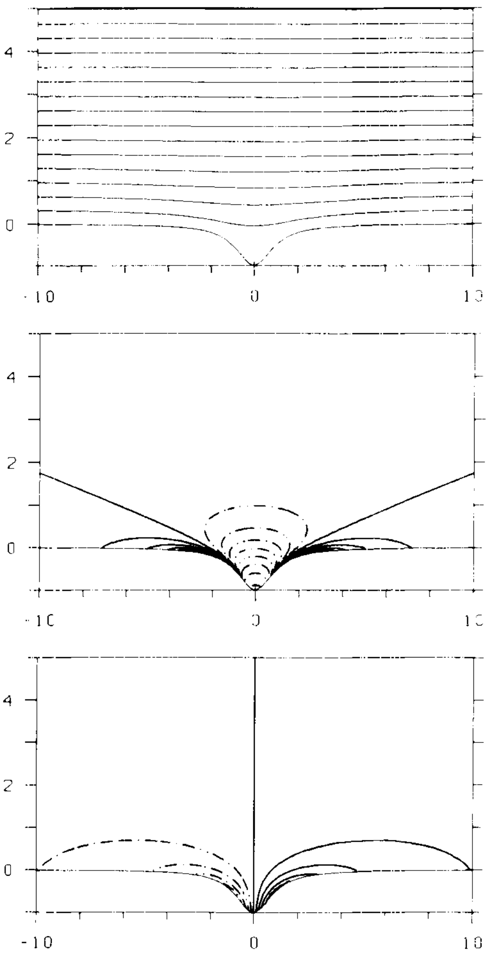

Fig. 2. As in Fig. 1, but for an inverted Witch of Agnesi orographic profile with $R_0\mathcal{F} = 5$ (Breakdown occurs at $R_0\mathcal{F} = 8$). The intervals of the velocity isolines is set at 0.1.

This problem was encountered by Eliassen and Thorsteinsson (1984) who adopted the latter approach coupled with orogenesis in the intial phase of their simulation. Our solution is not inconsistent with their result of approximate symmetry of mass outflow through up- and downstream boundaries during the initial stage and also with the slow decrease of the along ridge flow component with increasing distance from the orography. This however is a feature of our steady state solutions and therefore is not directly related to a dispersive effect of the initial transient wave pulse. Our solutions would also indicate a mass loss in the model domain equal to the mass of air replaced by the mountain and hence this is not consistent with the balanced Coriolis force contributing to an effective mass surplus in the domain.

3.2. *An "arc-tan" composite orography*

In this case, we consider an orographic shape that is a composite of two arc-tan profiles. It takes the form

$$\tilde\eta = (1/\pi)\{\tan^{-1}[(\tilde x + 1)/a] - \tan^{-1}[(\tilde x - 1)/a]\}. \quad (3.6)$$

This choice of profile allows us to examine furthei the sensitivity of the flow solutions to the shape and in particular to the curvature of the ridge slopes. Note that for $a \sim 1$ the profile is qualitatively similar to the bell-shaped profile of the previous case, whilst in the two limits $a \gtrsim O(1)$ and the $a \to O$ case, the profiles correspond respectively to broader smaller ridges, and steep-sloped top-hat configurations. It is pertinent to note that the height and length scales (H^* and L^*) implicit in eq. (3.6) do not in general correspond with the crest height and orographic half width. For convenience we shall define an $R_0^\bullet$ and an $\mathcal{F}^*$ based upon these new length scales whilst R_0 and $\mathcal{F}$ retain their original interpretation. The quantitative relationship between $(R_0^\bullet \mathcal{F}^*)$ and $(R_0 \mathcal{F})$ will be outlined where appropriate.

The expression for flow field structure for this composite orography are given by,

$$\tilde\varphi = (1/\pi) \times \{\tan^{-1}[(\tilde x + 1)/\tilde a] - \tan^{-1}[(\tilde x - 1)/\tilde a]\}. \quad (3.7)$$

$$\tilde v = (1/2\tilde a\pi) \times \mathcal{F}^* \ln\{[\tilde a^2 + (\tilde x + 1)^2]/[\tilde a^2 + (\tilde x - 1)^2]\}, \quad (3.8)$$

$$\tilde u = \langle 1 - (1/\pi)\, R_0^\bullet \mathcal{F}^* \{(\tilde x + 1)/[\tilde a^2 + (\tilde x + 1)^2] - (\tilde x - 1)/[\tilde a^2 + (\tilde x - 1)^2]\}\rangle^{-1} \quad (3.9)$$

with

$$\tilde a = a + (R_0^\bullet \mathcal{F}^*)\,\tilde\theta.$$

It can be shown (see 3.9) that for $a \gtrsim O(1)$ flow breakdown occurs at the crest for $(R_0^\bullet \mathcal{F}^*) = \pi(1 + a^2)/2$, corresponding to $(R_0 \mathcal{F}) \sim \sqrt{2}$ for $a \gg 1$. For $a = 1$ the precise rescaled criterion is $(R_0 \mathcal{F}) = \pi/(2\sqrt{2}) \sim 1.11$. For the sharper-sloped top hat configuration that pertain as a decreases from 1 toward 0, the point(s) of flow breakdown drift monotonically from the crest to the vicinity of $\tilde{x} = \pm 1_{\mp}$. In the limit $a \ll 1$, the breakdown criterion reduces to $(R_0^* \mathscr{F}^*) \sim (R_0 \mathscr{F}) \sim 2\pi a$ and occurs near $\tilde{x} = \pm(1-a)$. Thus in the high curvature limit $a \to 0$ the breakdown occurs for any finite value of $(R_0 \mathscr{F})$. This conclusion is in agreement with Eliassen's (1980) finding of a zero "critical crest height" if $\tilde{\eta}_{\tilde{x}\tilde{x}}$ does not exist even at one point.

The sensitivity of the flow response to the curvature values is a reflection of a relationship that is implicit in eq. (2.7). This indicates that at the surface the curvature of the orographic profile $(\tilde{\eta}_{\tilde{x}\tilde{x}})$ forces the value of $\varphi_{\tilde{\theta}\tilde{\theta}}$ (or equivalently $z_{\theta\theta}$). Thus it is apparent that the profile shape in addition to the parameter $(R_0 \mathscr{F})$ can play a significant rôle in determining the semi-geostrophic flow response.

In Figs. 3 and 4, the structure of the flow response is shown respectively for values of $\{R_0 \mathscr{F} = 1.1, a = 1.0\}$ and $\{R_0 \mathscr{F} = 0.5, a = 0.1\}$ corresponding in both cases to a "near-breakdown" flow regime. Both the terrain profile and the flow response in the first case (Fig. 3) resembles the solution for the Witch of Agnesi (see Fig. 1). The only perceptible difference is the stronger confinement of the along ridge flow component to lower levels. This is an indication

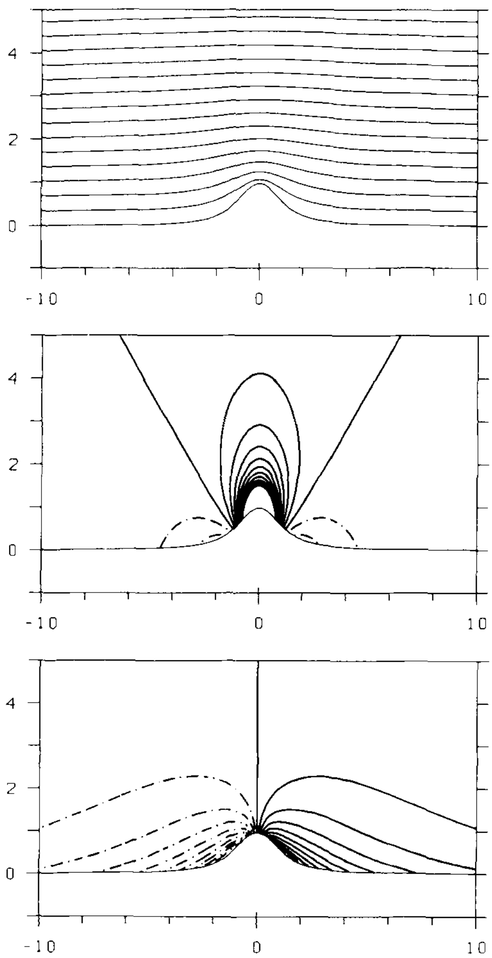

Fig. 3. As in Fig. 1, but for an arc-tan composite orography with $a = 1$ and $R_0 \mathscr{F} = 1.10$. (Breakdown occurs at $R_0 \mathscr{F} = 1.11$.)

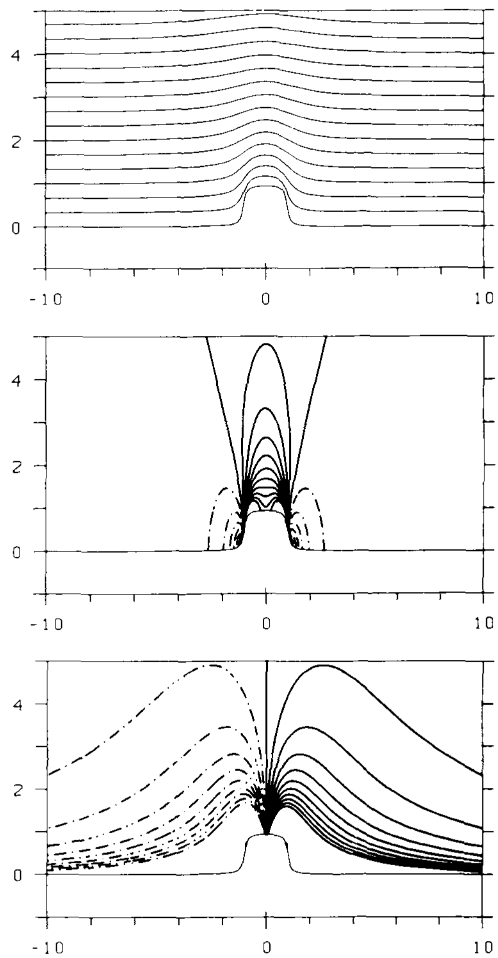

Fig. 4. As in Fig. 1, but for an arc-tan composite orographic profile with $a = 0.1$ and $R_0 \mathscr{F} = 0.50$. (Breakdown occurs at $R_0 \mathscr{F} \sim 0.63$.)

that the subtle difference in the orographic profiles in particular the slightly higher amplitude of the small wavelength components of the composite arc-tan profile, suffice to induce this vertical confinement.

In this respect, it is pertinent to note that the triangular shaped orography considered in P requires large amplitude of the smallest wavelength component and it is this that forces a singularity in the vertical structure.

The isentropic distribution of Fig. 4 reveals only mild upstream deacceleration of the incident flow field and this is confined to a comparatively small domain at the foot of the ridge. Maximum cross ridge flow now occurs at the edges of the plateau, and this is consistent with the large negative values of $\tilde{\eta}_{\tilde{x}\tilde{x}}$ at these locations. There is an accompanying strengthening of the along ridge flow component.

The displayed v field is (see eq. 3.5) the integrated response to the mild retardation over a long upstream reach and strong acceleration over a shorter distance in the immediate neighbourhood of the ridge itself.

3.3. *The asymmetric ramp orography*

The orographic profile

$$\tilde{\eta} = \tilde{x}/(1 + \tilde{x}^2)$$

is a simple example of an asymmetric terrain configuration. It corresponds to a valley-ridge profile, with a trough/ridge of height $\mp 1/\alpha$ located at $\tilde{x} = \mp 1$.

In this case, the flow response is given by,

$$\tilde{\varphi} = \tilde{x}/(\delta^2 + \tilde{x}^2), \tag{3.10}$$

$$\tilde{v} = \mathscr{F}\delta/(\delta^2 + \tilde{x}^2), \tag{3.11}$$

$$\tilde{u} = \{1 - 2(R_0\mathscr{F})\,\delta\tilde{x}/(\delta^2 + \tilde{x}^2)^2\}^{-1}, \tag{3.12}$$

with δ defined as before. Now the criterion for the existence of a finite flow response is

$$(R_0\mathscr{F}) < 8/3\sqrt{3} \sim 1.54.$$

The flow breakdown first occurs at $\tilde{x} = 1/\sqrt{3}$, i.e. between $\tilde{x} = 0$ and the ridge crest. An intriguing feature of the flow is that the flow component directed along the orography is always positive. There is an accompanying uniformly non-negative across-ridge pressure gradient and different pressure values far up- and down-stream. Thus an individual fluid element experiences only a positive deflection along the orography as it traverses the valley-ridge terrain. Nevertheless there is no accompanying net pressure force on the orography in the x-direction, since the negative drag on the valley portion of the orography ($\tilde{x} < 0$) is exactly offset by the positive drag on the ridge region ($\tilde{x} > 0$). This result is in harmony with theoretical expectation that the net Coriolis-related pressure force/lift is proportional to the mountain volume.

Fig. 5 illustrates the structure of the flow for $(R_0\mathscr{F}) = 1.5$. Again there is evident enhancement of the cross-ridge flow component in the region of strong negative orographic curvature, and this far surpasses the reduction of the flow component at

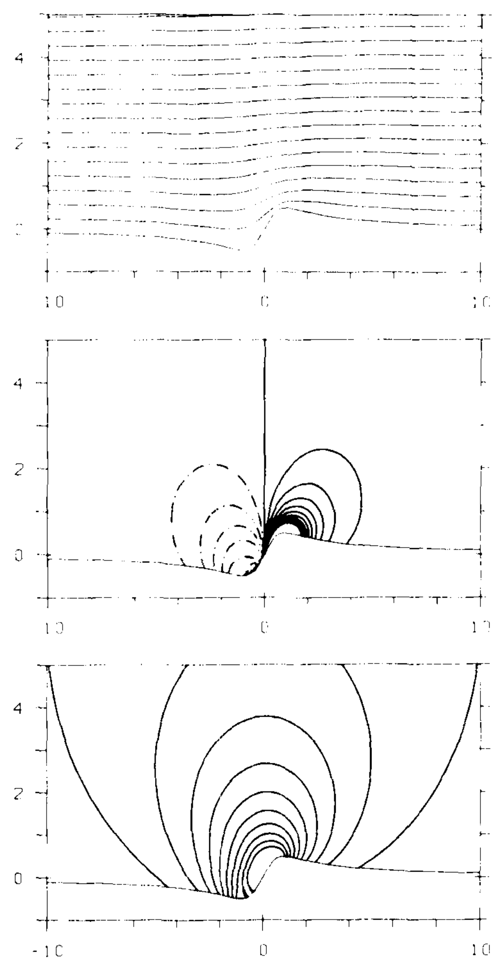

Fig. 5. As in Fig. 1, but for the asymmetric ramp orographic profile with $R_0\mathscr{F} = 1.50$. (Breakdown occurs at $R_0\mathscr{F} \sim 1.54$.)

the base of the sharp incline. The "along-the-orography" component with $\tilde{v} \equiv \mathscr{F}$ at $(\tilde{x}, \tilde{\theta}) = (0,0)$ can clearly be substantial. Finally note that the same structure prevails (except for the reversal in sign of v) if the flow approaches from the right and experiences a ridge-valley profile.

4. Flow over elongated valley-ridge orography

Now consider the issue of flow over elongated but finite length valley-ridge terrain. Our strategy is again to adopt a semi-geostrophic assumption and to assume geostrophy for the flow component that is aligned along the elongated axis of the orography. It then proves feasible, using the technique outlined in Section 2, to adapt *some* of our previous solutions to this new problem. To pinpoint the cause for this restriction imposed on the extension of the results of the previous section it is useful to record some of the results obtained using the quasi-geostrophic Boussinesq set of equations.

In this limit flow over a circularly symmetric bell-shaped mountain,

$$\tilde{\eta} = 1/[\tilde{x}^2 + \tilde{y}^2 + 1]^{3/2}$$

takes the following form at the surface (see e.g. Buzzi and Speranza, 1979; Smith, 1979b),

$$\tilde{u} = 1 + (\mathscr{F}\Lambda)\tilde{y}, \qquad \tilde{v} = -(\mathscr{F}\Lambda)\tilde{x},$$

where

$$\Lambda = [\tilde{x}^2 + \tilde{y}^2 + 1]^{-3/2}.$$

There is a Taylor cone provided

$$\mathscr{F} > 3\sqrt{3}/2 \sim 2.5.$$

Note that in the far-field, the mountain-induced perturbed geostrophic stream function is well behaved with $\varphi \propto 1/r$. In contrast for the flow over an infinite ridge aligned along the y axis and the induced v velocity at the ground is given by (see e.g. Smith, 1979b),

$$\tilde{v} = -\mathscr{F}\tilde{x}/(\tilde{x}^2 + 1),$$

and the far field stream function displays a logarithmic singularity.

This singularity is also a feature of the Montgomery stream function for the Witch of Agnesi and "Arc-tan Composite" solutions presented in subsections (3a,b). In mathematical terms the Fourier transform procedures for deriving our solutions correspond basically to taking the convolution product $\tilde{\eta} \times (R_0\mathscr{F})\tilde{\theta}/[(R_0\mathscr{F}\tilde{\theta})^2 + \tilde{x}^2]$, which according to the Lebesque Rule shows a far-field behaviour of $\varphi \propto 1/\tilde{x}^2$ for any $\tilde{\eta}$ with the integral $\int_{-\infty}^{\infty} \tilde{\eta} dx \neq 0$. In effect, the vorticity dynamics requires, for a non zero-volume orography, a far-field $1/|\tilde{x}|$ spatial decay of the along ridge flow. This in turn implies an along-ridge displacement of an infinite air mass but this airmass has to traverse a finite length orography. Thus it proves necessary because of this feature to restrict our consideration to orography with a zero net-volume.

One inference derivable from this zero net-volume requirement is that the flow system will not exert a net lift-force on the orography. However, this does not imply (c.f. Subsection 3.3) that there is no net-mean flow in the along-ridge direction.

To illustrate the nature of the three-dimensional flow response, we consider the following orographic profile,

$$\tilde{\eta}(\tilde{x}, \tilde{y}) = \left\{ \frac{(\tilde{x} + d)}{[1 + (\tilde{x} + d)^2]} - \frac{(\tilde{x} - d)}{[1 + (\tilde{x} - d)^2]} \right\} \times \frac{1}{(1 + \tilde{y}^2)}. \tag{4.1}$$

Thus in the x-direction the profile constitutes a superposition of two ramp profiles (c.f. eq. 3.12) of opposite sign and these are displaced distances $\pm d$ from the origin. The choice of the y-dependency of the profile is limited only by a "smoothness" requirement. For simplicity we have chosen the usual Witch of Agnesi shape. The value of d is set to 0.5, and we can recover an unit height and width terrain by rescaling (x, z) by respectively $(0.6^{-1}, 0.8^{-1})$. The height contours of the resulting orography are shown in Fig. 6 for the anisotropy parameter $R_L = 5$. Note that the central ridge is bordered by parallel small amplitude valleys at $x \sim \pm 2$, but the overall profile along the x-axis is not dissimilar to the simple symmetric profiles displayed in Figs. 1, 3.

Use of the equations (3.10–3.11) together with (2.11) provides the following solution set for the flow over the terrain given by (4.1),

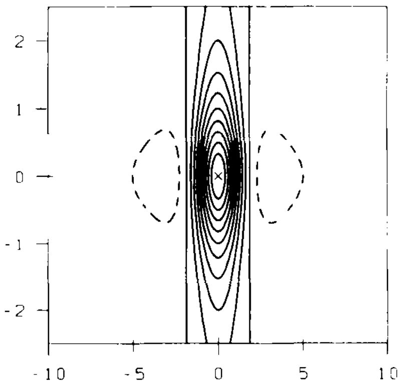

Fig. 6. Height contours of the three-dimensional orographic profile of (eq. 4.1). Contours displayed at intervals of 0.1. The dashed line corresponds to the height of -0.1. (Note that in dimensionless space, the central ridge is nearly circular and bordered by small amplitude valleys at $x \sim \pm 2$). The displayed scaling in the x- and y-directions takes into account the anisotrophy parameter $R_L = 5$. Here, and in all other figures, a further normalized rescaling to a unit height and a unit width has also been performed.

$$\varphi(\tilde{x}, \tilde{y}, \tilde{\theta}) = \left\{ \frac{(\tilde{x}+d)}{[\delta^2 + (\tilde{x}+d)^2]} - \frac{(\tilde{x}-d)}{[\delta^2 + (\tilde{x}-d)^2]} \right\} \times \frac{1}{(1+\tilde{y}^2)}, \tag{4.2}$$

$$\tilde{m}(\tilde{x}, \tilde{y}, \tilde{\theta}) = -(\mathscr{F}^*/R_0^*)\left\{ \tan^{-1}\left(\frac{\delta}{\tilde{x}+d}\right) - \tan^{-1}\left(\frac{\delta}{\tilde{x}-d}\right) \right\} \times \frac{1}{(1+\tilde{y}^2)}, \tag{4.3}$$

$$\tilde{v}(\tilde{x}, \tilde{y}, \tilde{\theta}) = \mathscr{F}^*\delta\{[d^2 + (\tilde{x}+d)^2]^{-1} - [\delta^2 + (\tilde{x}-d)^2]^{-1}\} \times \frac{1}{(1+\tilde{y}^2)}, \tag{4.4}$$

$$\tilde{u}(\tilde{x}, \tilde{y}, \tilde{\theta}) = \left\langle 1 - 2(R_0^*\mathscr{F}^*)\,\delta \left\{ \frac{(\tilde{x}+d)}{[\delta^2 + (\tilde{x}+d)^2]^2} - \frac{(\tilde{x}-d)}{[\delta^2 + (\tilde{x}-d)^2]^2} \right\} \frac{1}{(1+\tilde{y}^2)} \right\rangle \times \left\langle \sin\alpha + (R_0^*/R_L)\frac{2\tilde{y}}{(1+\tilde{y}^2)^2} \times \left\{ \frac{1}{(1+\tilde{y}^2)}\tilde{v} + \tilde{m} \right\} \right\rangle. \tag{4.5}$$

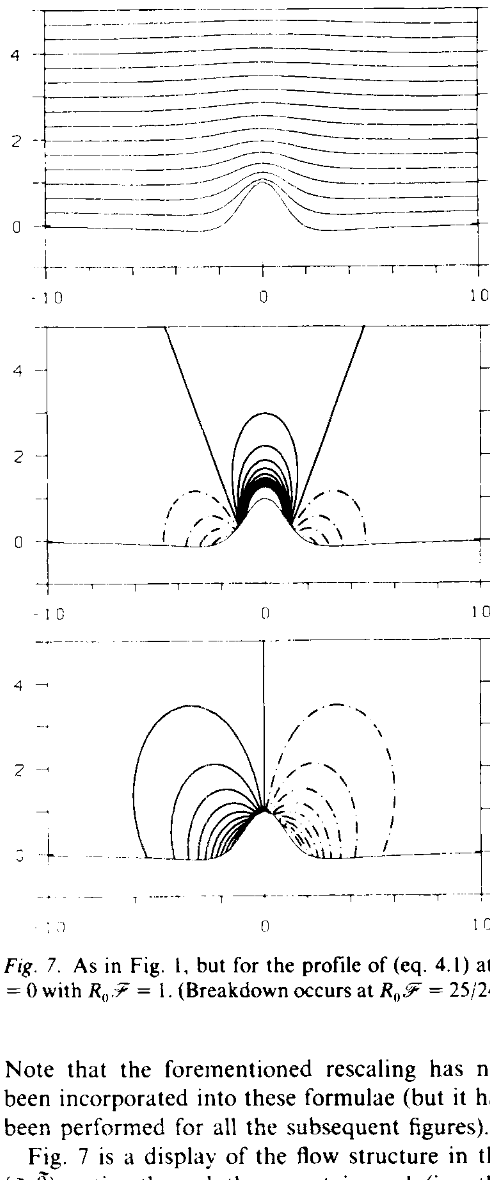

Fig. 7. As in Fig. 1, but for the profile of (eq. 4.1) at $\tilde{y} = 0$ with $R_0\mathscr{F} = 1$. (Breakdown occurs at $R_0\mathscr{F} = 25/24$).

Note that the forementioned rescaling has not been incorporated into these formulae (but it has been performed for all the subsequent figures).

Fig. 7 is a display of the flow structure in the $(\tilde{x}, \tilde{\theta})$ section through the mountain peak (i.e., the $\tilde{y} = 0$ plane) for $(R_0\mathscr{F}) = 1$. The patterns generally resemble those for bell-shaped orography (Fig. 1), and this suggests that the shallow side valleys do not induce significant aberrant behaviour. Also the breakdown criterion $(R_0\mathscr{F}) = 25/24$ is commensurate with the previous results of subsections 3.1, 3.2. Now however, the three-dimensionality of the flow implies that the isentropes are no longer streamlines, and there are important differences in the far field structure of $\tilde{m}$ and $\tilde{v}$.

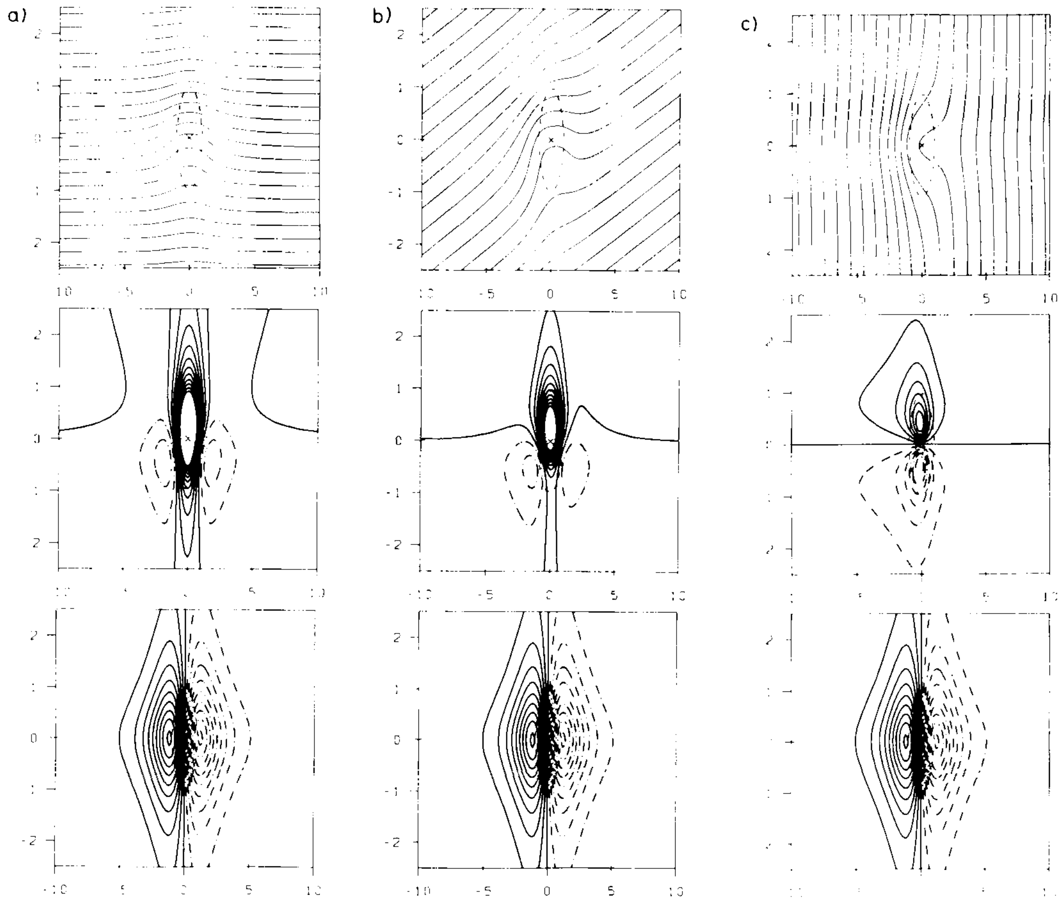

Fig. 8. Depiction of the horizontal distribution of the ground-level flow for $R_0 = 0.6$, $\mathscr{F} = 0.6^{-1}$, $R_L = 5$. The angle α takes the respective values (a) $\alpha = \pi/2$, (b) $\alpha = \pi/4$ and (c) $\alpha = 0$, corresponding to normal incidence, an intermediate angle of attack and grazing incidence. The displayed equidistant isolines are of the mass flux stream function ψ. In successive panels, the flow approaches from the left and from the bottom, respectively. Positive u- and v-values relate to flow from the left (middle panels) and from the bottom (lower panels), respectively. The dashed ellipse corresponds to the "half-height" contour of the mountain. Velocity isolines are displayed at intervals of 0.1 up to 2.0 and dashed isolines correspond to negative perturbations.

A horizontal view of the flow at the ground is shown in Fig. 8 for $R_0 = 0.6$; $\mathscr{F} = 0.6$ and $R_L = 5$. Here the isolines are that of the mass-flux stream function, ψ. The generation of anticyclonic circulation over the terrain is clearly evident. A Taylor cone will form if the accompanying vorticity is strong enough to develop a stagnation point in the flow. This requires $(\tilde{u}, \tilde{v}) = (0,0)$ somewhere, and from (2.11) this is equivalent to the following condition

$$\sin \alpha = (R_0/R_L)^{-1} \tilde{M}_{\tilde{y}}. \qquad (4.6)$$

To explore these relationships further let us, for simplicity, consider a mountain with circular contours (this is a not unreasonable qualitative assumption for our non-dimensionalized terrain in the regions of large terrain slope).

Let $\tilde{M}$ take the form (c.f. eq. 4.3),

$$\tilde{M}(\tilde{x}, \tilde{y}, \tilde{\theta}) = -\tfrac{1}{2}\mathscr{F}^2\theta^2 - \mathscr{F} R_0^{-1}\, g(\tilde{r}, \tilde{\theta}),$$

where

$$\tilde{r}^2 = \tilde{x}^2 + \tilde{y}^2$$

Then the stagnation point criterion (4.6) reduces to

$$\sin\alpha + (R_L)^{-1}(\tilde{y}_0/\tilde{x}_0)\cos\alpha = 0, \quad (4.7)$$

with $(\tilde{y}_0/\tilde{x}_0)$ referring to the direction from the origin of the stagnation point. This expression can be recast in the form

$$\sin\alpha + (R_L)^{-1}\mathscr{F}[1 + (R_L)^{-2}\cot^2(\alpha)]^{-1/2} \times g' = 0, \quad (4.8)$$

where g' denotes the derivative of g with respect to $\tilde{r}$. Thus an incipient Taylor cone first occurs at a point where $g'(\tilde{r},\tilde{\theta})$ has a maximum (say, $g' = G$). It follows that for a circular profile the flow will possess a Taylor cone if

$$\mathscr{F} > \mathscr{F}_{crit} = -(1/G)[\cos^2\alpha + (R_L)^2\sin^2\alpha]^{1/2}. \quad (4.9)$$

This criterion is also reasonably accurate for our terrain profile. Furthermore it bears out the fact that the strength of the mountain induced anticyclone is dependent upon the Froude number (and not the Rossby number) of the incident stream.

The newly derived Taylor cone criterion (4.9) is to be compared with the $\mathscr{F} > 3\sqrt{3/2}$ criterion quoted earlier for quasi-geostrophic flow over a circularly symmetric obstacle. Fig. 9 is a portrayal of the relationship (4.9). It indicates that, for flow

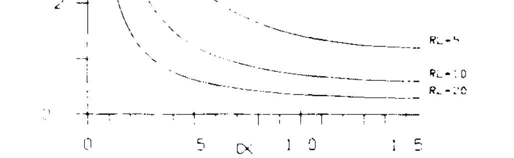

Fig. 9. The Taylor Cone criterion (see eq. 4.9, but displayed in terms of the Froude number F rather than the inverse Froude number $\mathscr{F}$) is shown for the following values of the anisotropy parameter $R_L = \{1, 5, 10, 20\}$. A set value of $G = 0.6$ is chosen for m varying between 0.55 and 0.65, depending on the direction of taking $\partial g/\partial r$. For a given R_L-value, no Taylor cone can form above the isoline for that value.

over elongated topography (i.e., $R_L \gg 1$), the occurrence of a Taylor cone is favoured by large values of $\mathscr{F}$ (i.e., small values of U/NH) and almost along-ridge incident flow. (Indeed in the limit of $R_L^{-1} \to 0$, only acute-angled incident flow ($\alpha \to 0$) can satisfy the criterion).

A set of flow solutions are shown in Fig. 10 for parameter values that satisfy the Taylor cone criterion. Normal incidence (Fig. 10a) is associated with only a weak cone, whilst an incident flow of the same strength but at an acute angle of attack (Fig. 10c) is associated with a much stronger closed circulation. In Fig. 11 the flow response is shown for the same parameter setting as Fig. 10, but now with $R_L = 10$. There is no cone formation in the normal incidence case and this result is in agreement with the criterion (4.9).

Now let us examine one measure of the validity of these semi-geostrophic three-dimensional flow solutions. Consider the ratio,

$$E(\tilde{x},\tilde{y},0) = |uu_x + vu_y|/|fv|. \quad (4.10)$$

The horizontal spatial distribution of $E(\tilde{x},\tilde{y},0)$ is shown in Fig. 12 for various different sets of parameter values. This ratio decreases both with the Rossby number and the inverse of the anisotropy parameter (R_L). In the limit of $R_L^{-1} \to 0$ the values naturally drop to those obtained in the two-dimensional studies. Also E exhibits a dependency upon the angle of attack α, with incident flow parallel to the mountain associated with smaller E values.

Finally note that, as before, the derived solution (4.2–4.5) will also apply for flow over a trench. A reversal of the sign for the orographic profile (4.1) reverses the sign of $\tilde{\varphi}$, $\tilde{m}$ and $\tilde{v}$. The changes in the ũ field are less trivial. An example of the flow response to a trench is presented in Fig. 13. The general appearance is consistent with the reversed two-dimensional ridge profile of Fig. 2. For this case of reversed profile the flow breakdown criterion is much higher, $(R_0\mathscr{F}) \sim 3.3$, with a commensurate lowering of the values of E, the credibility measure.

5. Further remarks

The cornerstone of the present study is the adoption of the semi-geostrophic assumption with geostrophy prescribed for the along-ridge flow

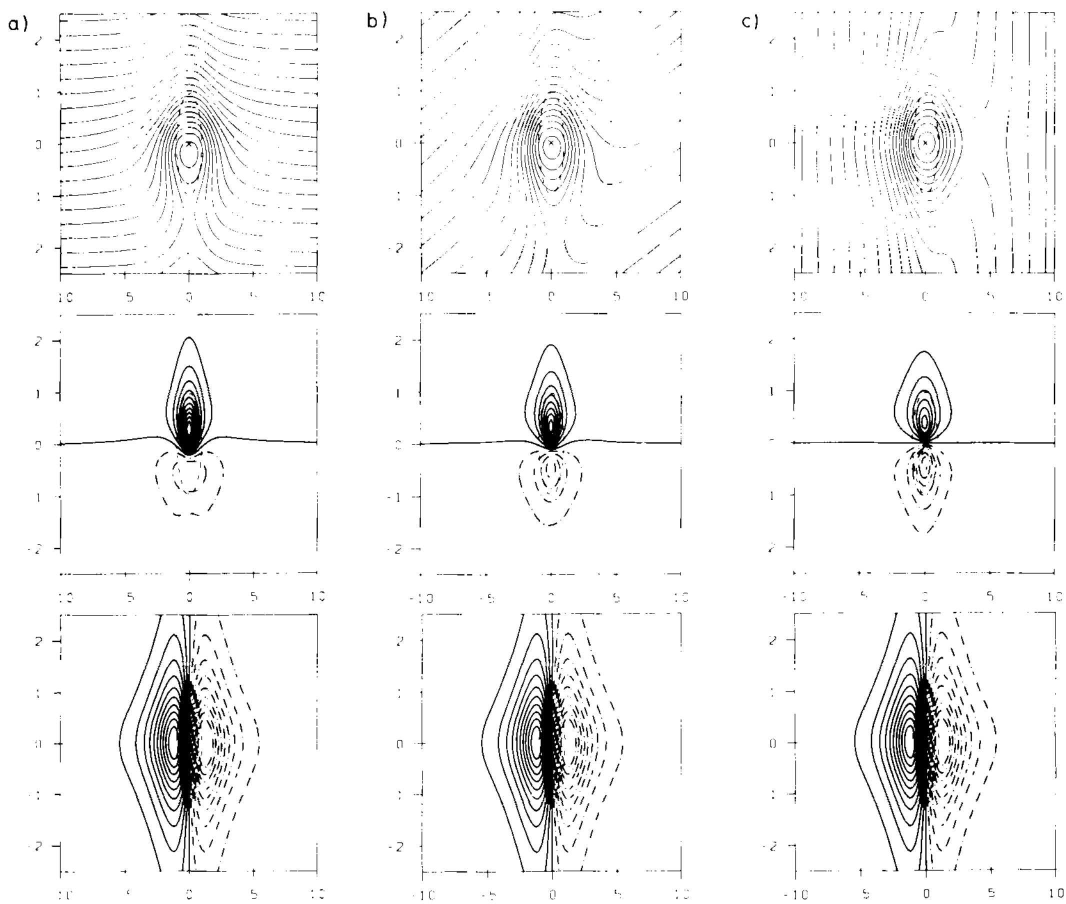

Fig. 10. As in Fig. 8, but for $R_0 = 0.1$, $\mathscr{F} = 0.1^{-1}$, $R_L = 5$ and with velocity-isoline intervals of 0.5.

component. This represents a reasonable heuristic approach to the examination of the nature and amplitude of the strongly ageostrophic, yet balanced, flow response that can occur in the $R_0 \to 1$ limit. The resulting flow solutions served to illustrate that the "physical breakdown" of the semi-geostophic flow is sensitively dependent both upon the dimensionless Rossby radius of deformation ($R_0 \mathscr{F} = NH/fL$) and upon the orographic shape. For smooth orographic profiles the breakdown occurred for $R_0 \mathscr{F} \sim 1$, but for a profile with high convex curvature this value reduces considerably. The formal "mathematical-breakdown" of the semi-geostrophic assumption, based upon the credibility measures E (see eqs. (3.4) and (4.10)), occur for values of $(R_0 \mathscr{F})$ that are much lower than those that pertain for physical-breakdown.

Thus in seeking to apply these results to the major geophysical sub-synoptic/ meso-α scale mountain ranges the solution derived herein prove in a sense to be self-limiting. Consider for instance the relation (see eq. (3.4))

$$E(0,0) = 6R_0^2(1 - R_0 \mathscr{F})^{-3}$$

that is valid for the infinite-length, Witch of Agnesi ridge. For typical mid-latitude values of U, N, and f then

$$R_0 \sim (5\text{–}10) \cdot 10^4/L, \qquad \text{and} \qquad R_0 \mathscr{F} = (H/L)\, 10^2.$$

Thus a requirement of the form $E \ll 1$ would imply that the theory was applicable only for mountain half widths with $L \gg (100\text{–}250)$ km and orographic aspect ratios with $(H/L) \ll 10^{-2}$. *The inference in*

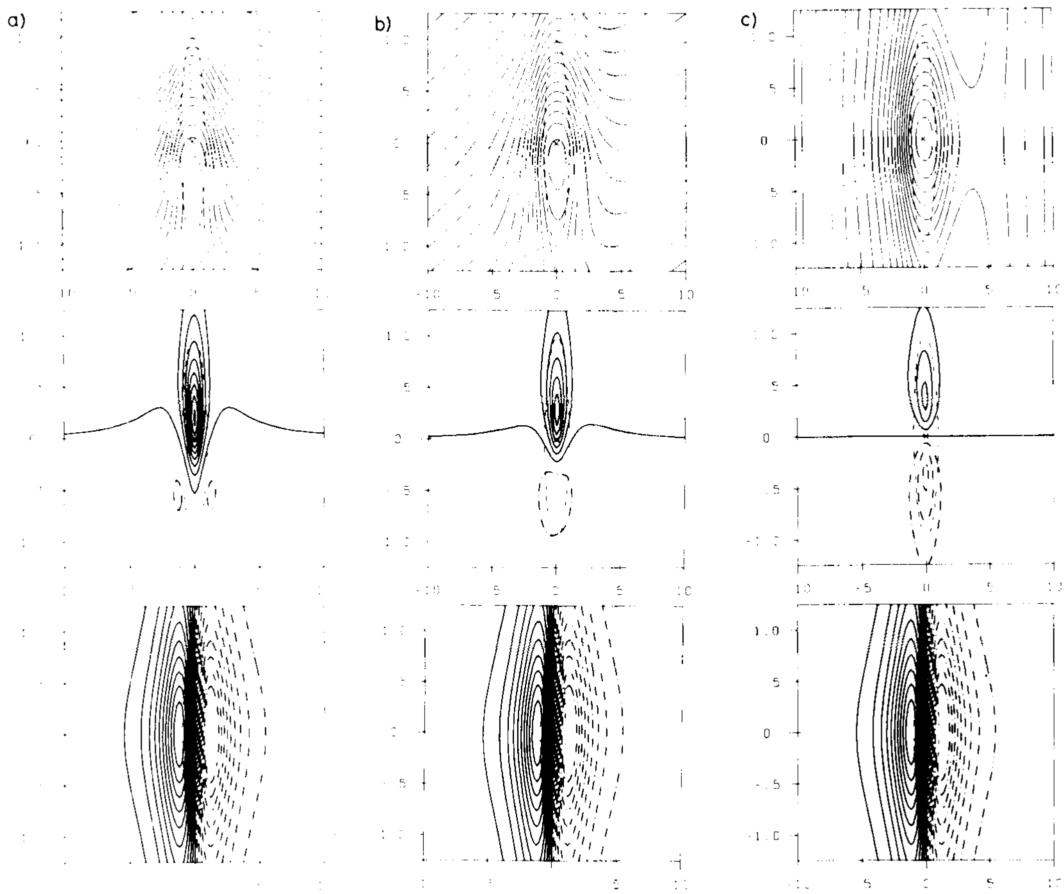

Fig. 11. As in Fig. 8, but for $R_0 = 0.1$, $\mathscr{F} = 0.1^{-1}$, $R_L = 10$ and with velocity-isoline intervals of 0.5. The different value of R_L implies that the scaling of the dimensionless x-unit in these plots differs from that of Fig. 8 and 10.

this case is that for typical adiabatic flow incident almost normally upon a ridge, then ageostrophic buoyancy waves, and/or low-level upstream blocking, and/or three-dimensional effects, must assume a significant role for sub-synoptic and meso-α scale mountains of even moderate height. Here we offer some further comments upon these various possibilities.

Some insight to the possible generation and role of ageostrophic buoyancy waves can be gleaned by considering the nature of the residual flow forced by the semi-geostrophic flow. The theoretical outline for such an approach is presented in the Appendix where it is qualitatively argued that buoyancy waves forced by the semi-geostrophic flow would:

(i) tend to counteract the occurrence of the surface flow breakdown associated with the pure semi-geostrophic response;

(ii) the vertical propagation of those forced waves out of the surface regions of high wind speed would result in the generation aloft of local regions of large $M_{\theta\theta}$ (i.e. essentially small static stability).

These qualitative and highly speculative inferences regarding the nature of the forced ageostrophic response need further substantiation, but they do point to the possible translation of the phenomenon of flow breakdown from a surface based direct semi-geostrophic effect to a higher level ageostrophic wave overturning.

This interpretation is not at variance with the

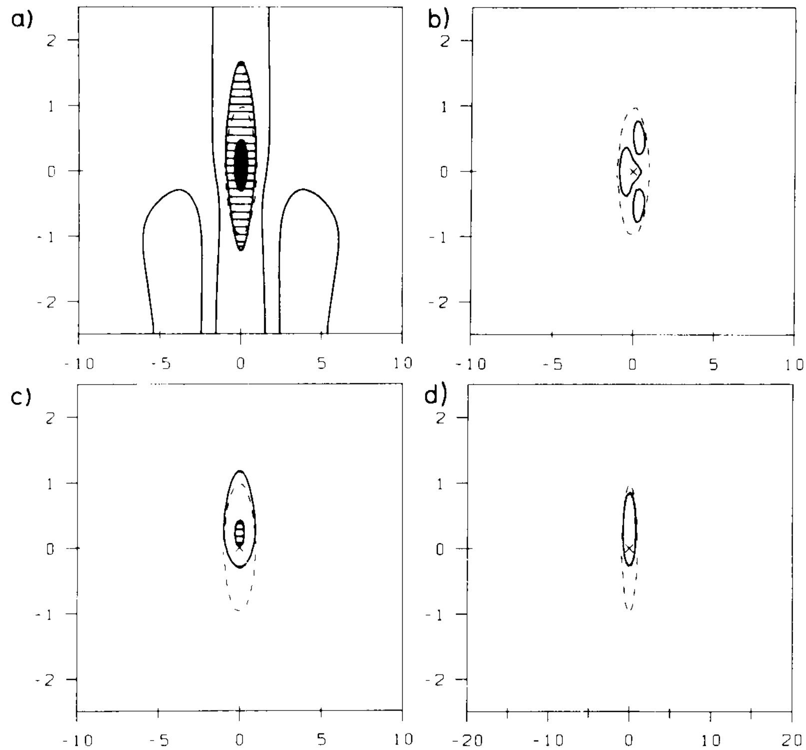

Fig. 12. Horizontal spatial distribution of the credibility measure $E(\tilde{x}, \tilde{y}, 0)$ for (a) $R_0 = 0.6$, $\mathscr{F} = 0.6^{-1}$, $R_L = 5$, $\alpha = \pi/2$; (b) $R_0 = 0.6$, $\mathscr{F} = 0.6^{-1}$, $R_L = 5$, $\alpha = 0$; (c) $R_0 = 0.1$, $\mathscr{F} = 0.1^{-1}$, $R_L = 5$, $\alpha = \pi/2$ and (d) $R_0 = 0.1$, $\mathscr{F} = 0.1$, $R_L = 10$, $\alpha = \pi/2$. The isolines delimit the areas where $E > 0.1$, $E > 1.0$ and $E > 10$ (black area).

results obtained by Pierrehumbert and Wyman (1985) using a two-dimensional primitive equation numerical model. They showed that in the $R_0 \mathscr{F} \sim 1$ domain large amplitude buoyancy waves were generated and that the breaking of these waves aloft coincided with, or occurred just prior to, the onset of low-level upstream blocking.

It is of some interest to note that the existence of a blocked region of substantial lateral width ahead of an elongated terrain would present the surmounting air with a ramp-like profile akin to that considered in Subsection 3.3.

The foregoing comments dealt exclusively with the two-dimensional flow response. In the consideration of the three-dimensional response other physical factors are present and these might supersede or override the significance of the strictly two-dimensional response. Here we comment on some of the limitations that are implicit in the solutions obtained in Section 4 for flow over three-dimensional isentropic terrain. In his classification of the various possible orographic flow configurations, Eliassen (1980) indicated that solutions with a non-isentropic, warm crest configuration might prevail under certain conditions. It is possible to envisage a semi-geostrophic orographic flow pattern with substantial deflection of the low-level air around the terrain surmounted by an upper flow regime characterized by a predominance of flow over the mountain. In this event the limited applicability of our present solutions might then be attributable to the enforcing of the isentropic lower boundary condition and not necessarily to the inappropriateness of the semi-geostrophic assumption. A related issue is the question (see Eliassen, (1980)) of the uniqueness of the "isentropic-closed" flow solutions derived in Section 4.

Finally we note that the severe contraints upon the validity of the semi-geostrophic assumption noted in this study combined with the possible existence of a strong buoyancy wave response, low

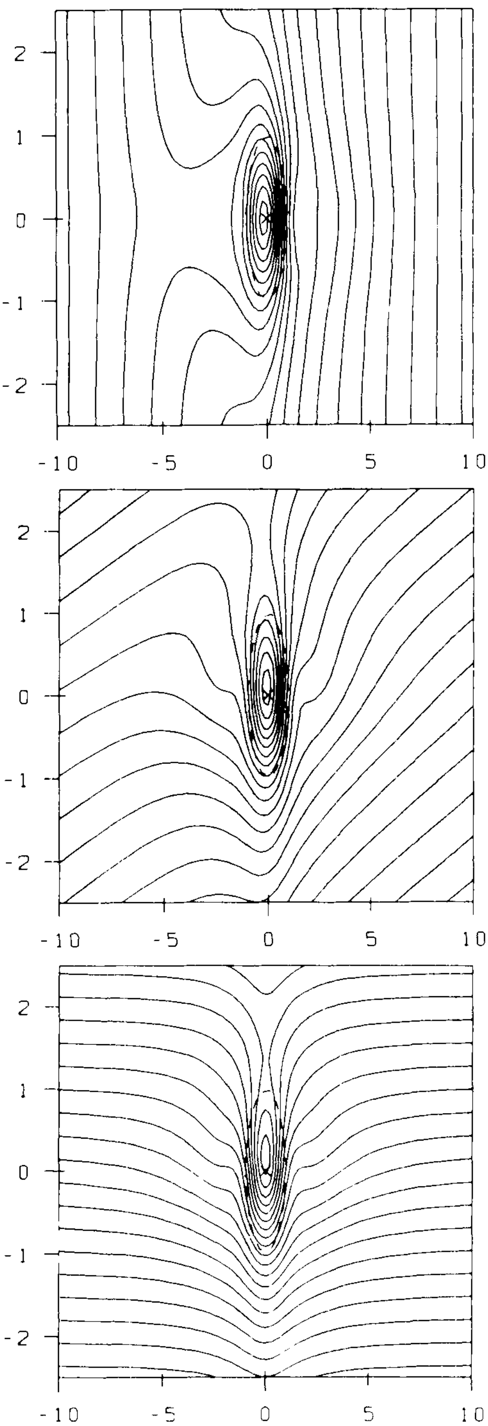

level upstream blocking and even non-uniqueness of the three-dimensional flow problem is of some direct concern in the context of numerical weather prediction. The various intialization techniques of NWP invoke, either explicitly or implicitly, an assumption of "balanced" flow. Thus it would be of interest to ascertain the nature of the initial state that these techniques would yield in the neighbourhood of high terrain features.

6. Acknowledgments

It is a pleasure to thank J. Müller for discussions that led to useful cross-fertilization of ideas, to Prof. W. Blumen for prompting us to examine more carefully the relationship between orographic curvature and flow breakdown, and to Prof. A. Eliassen for an incisive and helpful review of the work.

7. Appendix. Semi-geostrophic forcing of residual motion

Here we outline briefly a theoretical framework for examining the nature of the residual flow field forced by the semi-geostrophic response to a two-dimensional ridge.

Let the full flow field be decomposed in the form

$$(u, v, M, p) = (u_s, v_s, m_s, p_s) + (u', v', m', p').$$

Here the subscript 's' and the prime notation refer to respectively the semi-geostrophic and residual flow components, and $p = M_{\theta\theta}$. It follows that the full flow field satisfies the set (2.1) and the semi-geostrophic variables satisfy the set (2.2). Hence, the residual variables are governed by the resulting difference of these two sets of equations, viz.,

$$\begin{aligned} &u_s(u_s)_x + u_s u'_x + u'(u_s + u')_x - fv' = -m'_x \\ &u_s v'_x + u'(v_s + v')_x + fu' = 0 \qquad \text{(A.1)} \\ &u_s p'_x + u'(p_s + p')_x + p_s u'_x = -p'(u_s + u')_x. \end{aligned}$$

Fig. 13. Response to flow over a trench. Shown is the mass flux stream function at the ground with $R_0 = 0.4$, $\mathcal{F} = 0.1^{-1}$, $R_L = 5$, and α taking the respective values of $\alpha = \pi/2$, $\pi/4$ and 0. The slight deflections on both sides of the trench are caused by the small amplitude ridges present at those locations.

It can be deduced, on assuming that the residual flow variables are second order and their products negligible, that the behaviour of the residual flow is governed by the equation,

$$[(-u_s^3/\mathcal{M}_{\theta\theta}\mathcal{V})m'_{\theta\theta}]_{xx} - (f^2/\mathcal{M}_{\theta\theta})m'_{\theta\theta} + m'_{xx} = -\tfrac{1}{2}(u_s^2)_{xx}. \tag{A.2}$$

A full solution of this equation with appropriate boundary conditions would yield (at least in the linear limit) the form of the residual flow. Here we confine ourselves to some general remarks. First note that a further substantial simplification of (A.2) follows if it is assumed that the region of major semi-geostrophic forcing (i.e. the $\frac{1}{2}(u_s^2)_{xx}$ term) is characterized by a comparatively small horizontal scale. In this limit the response equation reduces to

$$m'_{\theta\theta} - (\mathcal{M}_{\theta\theta}/u_s^2)m' = -\tfrac{1}{2}\mathcal{M}_{\theta\theta}\left[\left(\frac{\mathcal{V}}{u_s}\right)^2 - 1\right]$$

with the boundary conditions

$$m'_\theta = 0 \quad \text{at} \quad \theta = 0,$$

and a radiation condition off at infinity.

In this form, the problem represents the hydrostatic, non-rotationally influenced, buoyancy wave response to the forcing. The semi-geostrophic flow influences this residual response in two ways. The departure of u_s from $\mathcal{V}$ determines the amplitude and location of the forcing, and the u_s structure also influences the vertical structure of the wave response. Finally, note that in regions of large u_s (and concomitantly small $(m_s)_{\theta\theta}$) the equation suggests the substantial pairing of the $m'_{\theta\theta}$ term with the $-\frac{1}{2}(m_s)_{\theta\theta}$ term. This would contradict the small perturbation assumption invoked earlier. However, the tendency implied by such a relationship lends itself to some interesting inferences. It suggests that buoyancy waves forced by the semi-geostrophic flow would counteract the low-level tendency for flow speed-up at the crest, and would concomitantly, by vertical propagation, induce substantial static stability changes aloft.

REFERENCES

Baines, P. G. and Hoinka, K.-P. 1985. Stratified flow over two-dimensional topography in a fluid of infinite depth: A laboratory simulation. *J. Atmos. Sci. 42*, 1614–1630.

Bannon, P. R. 1986. Deep and shallow quasi-geostrophic flow over mountains. *Tellus 38A*, 162–169.

Buzzi, A. and Speranza, A. 1979. Stationary flow of a quasi-geostrophic, stratified atmosphere past finite amplitude obstacles. *Tellus 31*, 1–12.

Buzzi, A. and Tibaldi, S. 1977. Inertial and frictional effects on rotating stratified flow over topography. *Q.J.R. Meteorol. Soc. 103*, 123–150.

Davies, H. C., Binder, P. and Furger, M. 1984. Dynamical considerations of Alpine upstream flow regimes. *Zbornik 10*, 43–46.

Davies, H. C. and Roth, K. 1986. Semigeostrophic response of shallow water flow incident upon slender orography. Part I: Flow over an elongated ridge. *Ann. Geophys. 4B*, 495–506.

Eliassen, A. 1968. On mesoscale mountain waves on the rotating earth. *Geofys. Publ. 27-6*, 1–15.

Eliassen, A. 1980. Balanced motion of a stratified, rotating fluid induced by bottom topography. *Tellus 32*, 537–547.

Eliassen, A. and Rekustad, J. E. 1971. A numerical study of mesoscale mountain waves. *Geofys. Publ. 28-3*, 1–13.

Eliassen, A. and Thorsteinsson, S. 1984. Numerical studies of stratified air flow over a mountain ridge on the rotating earth. *Tellus 36A*, 172–186.

Hogg, N. G. 1973. On the stratified Taylor column. *J. Fluid Mech. 58*, 517–537.

Huppert, H. E. 1975. Some remarks on the initiation of inertial Taylor columns. *J. Fluid Mech. 67*, 397–412.

Jacobs, S. J. 1964. On stratified flow over bottom topography. *J. Mar. Res. 22*, 223–235.

Mason, P. J. and Sykes, R. I. 1978. On the interaction of topography and Ekman boundary layer pumping in a stratified atmosphere. *Q.J.R. Meteorol. Soc. 104*, 475–490.

Merkine, L.-O. 1975. Steady finite amplitude baroclinic flow over long topography in a rotating stratified atmosphere. *J. Atmos. Sci. 32*, 1881–1893.

Merkine, L.-O. and Kalnay-Rivas, E. 1976. Rotating stratified flow over finite isolated topography. *J. Atmos. Sci. 33*, 908–922.

Pierrehumbert, R. T. 1984. Linear results on the barrier effects of mesoscale mountains. *J. Atmos. Sci. 41*, 1356–1367.

Pierrehumbert, R. T. 1985. Stratified semigeostrophic flow over two-dimensional topography in an unbounded atmosphere. *J. Atmos. Sci. 42*, 523–526.

Pierrehumbert, R. T. and Wyman, B. 1985. Upstream effects of mesoscale mountains. *J. Atmos. Sci. 42*, 977–1003.

Queney, P. 1947. Theory of perturbations in stratified currents with applications of airflow over mountain barries. Misc. Report No. 23, Dept. of Met., Univ. of Chicago, 81 pp.

Queney, P. 1948. The problems of airflow over mountains: A summary of theoretical studies. *Bull. Am. Meteorol. Soc. 29*, 16–26.

Robinson, A. R. 1960. On two-dimensional inertial flow in a rotating stratified fluid. *J. Fluid Mech. 9*, 321–331.

Smith, R. B. 1979a. The influence of the earth's rotation on mountain wave drag. *J. Atmos. Sci. 36*, 177–180.

Smith, R. B. 1979b. Some aspects of quasi-geostrophic flow over mountains. *J. Atmos. Sci. 36*, 2385–2393.